THE JOURNAL OF PHYSICAL CHEMISTRY Letters

Letter

pubs.acs.org/JPCL

Flexoelectricity in Carbon Nanostructures: Nanotubes, Fullerenes, and Nanocones

Alexander G. Kvashnin,[†,‡,§] Pavel B. Sorokin,*[,†,‡,∥] and Boris I. Yakobson*[,†]

[†]Department of Materials Science and NanoEngineering and the Smalley Institute for Nanoscale Science and Technology, Rice University, Houston, Texas 77005, United States

[‡]Technological Institute of Superhard and Novel Carbon Materials, Moscow 142190, Russian Federation

[§]Moscow Institute of Physics and Technology, Dolgoprudny 141700, Russian Federation

[∥]National University of Science and Technology MISiS, Moscow 119049, Russian Federation

ABSTRACT: We report theoretical analysis of the electronic flexoelectric effect associated with nanostructures of sp^2 carbon (curved graphene). Through the density functional theory calculations, we establish the universality of the linear dependence of flexoelectric atomic dipole moments on local curvature in various carbon networks (carbon nanotubes, fullerenes with high and low symmetry, and nanocones). The usefulness of such dependence is in the possibility to extend the analysis of any carbon systems with local deformations with respect to their electronic properties. This result is exemplified by exploring of flexoelectric effect in carbon nanocones that display large dipole moment, cumulative over their surface yet surprisingly scaling exactly linearly with the length, and with sine-law dependence on the apex angle, $d_{flex} \sim L \sin(\alpha)$. Our study points out the opportunity of predicting the electric dipole moment distribution on complex graphene-based nanostructures based only on the local curvature information.

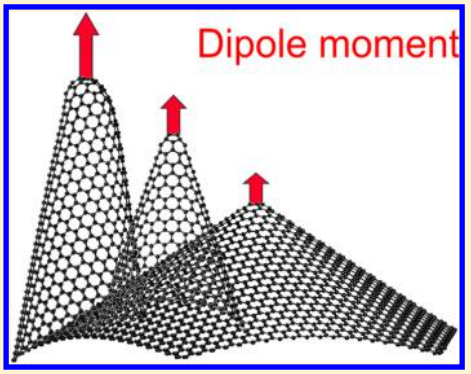

The discovery of freestanding graphene[1] promoted the extensive investigations of the properties of monolayered two-dimensional structures. An infinite graphene sheet displays no dipole moment (except the instantaneous quantum-fluctuative responsible for the van der Waals interactions). A homogeneous mechanical distortion of graphene also cannot induce electrical dipole due to graphene lattice central symmetry center (no piezoelectric effect). This rule, however, does not apply to the second-order electronic flexoelectric effect (EFE) induced by the strain gradient, especially by the bending of graphene sheet, which is one of the most intriguing properties of graphene. EFE is a unique feature associated with atomic monolayers, referring to the emergence of net of electric dipole moments in a deformed nonpolar two-dimensional (2D) system due to the mirror symmetry breaking which leads to charge redistribution. It has first been demonstrated for carbon nanotube (CNT), as a graphene sheet wrapped into a seamless cylinder, that the dipole moment of each charge-neutral atom is nonzero;[2] the total dipole moment of CNT however vanishes due to its cylindrical symmetry. It is expected that a small part of nanotube should display a significant local dipole moment. Nonzero total dipole moment of graphene can be obtained by nonsymmetrical distortion, for example, by the bending of the finite graphene piece.[3]

Graphene can naturally be considered as a building precursor for the family of previously discovered carbon shell structures, such as fullerenes, CNTs, nanoribbons, and nanocones, which all possess intriguing properties. One can expect that similar type of covalent bonding in these nanostructures should permit to describe their flexoelectricity in some common way.

Although the previous atomistic studies showed the linear dependence of atomic dipole moment on the local curvature in CNT with equivalent carbon atoms, the assessment of EFE in the structures with nonequivalent atoms remains unclear. On the other hand, such structures, including low symmetry fullerenes and nanocones, are gaining more interest.

In this paper, the universality of the linear dependence of flexoelectric dipole moments on the local curvature for different carbon networks with various atomic arrangements is established by combining direct ab initio calculations with, wherever possible, analytical phenomenological equations. Using the obtained universal flexoelectric coefficient, the large dipole moment values of various carbon nanocones are predicted and their scaling with cone dimensions is elucidated. We found a linear dependence of the total dipole moments of nanocones, of a given apex angle, on their lateral length. Our analysis suggests the possibility of predicting the electric dipole moments of complicated low-dimensional systems based on their geometry.

In the following, we first calculate the atomic dipole moments for structures with atoms equivalent by symmetry and then extend the approach to the structures with nonequivalent C atoms. Then the dipole moments of the

Received: May 19, 2015
Accepted: June 23, 2015

DOI: 10.1021/acs.jpclett.5b01041
J. Phys. Chem. Lett. 2015, 6, 2740−2744

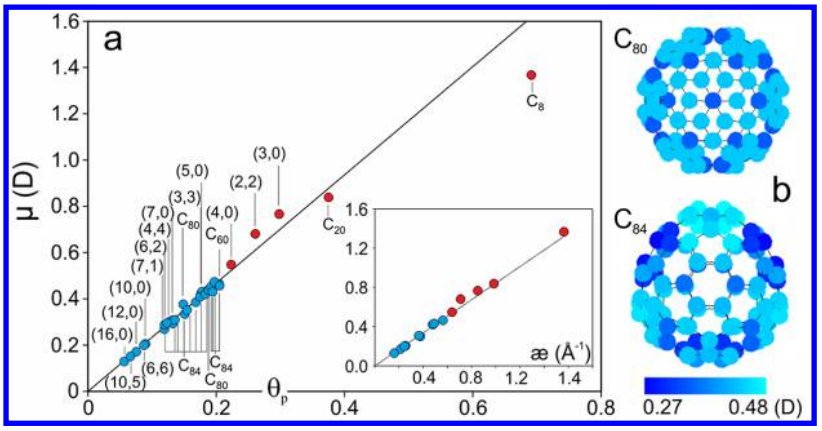

Figure 1. (a) Computed atomic dipole moments μ for carbon nanostructures as a function of pyramidalization angle θ_p and curvature (the inset shows dipole only for systems composed of equivalent atoms, where Gaussian curvature æ equals to $(1/R)$ in a case of nanotubes and $(2/R)$ in a case of fullerenes); red points indicate highly distorted structures which dipole moment deviates from the linear dependence. (b) Color distribution of atomic dipole moment values for C_{80} and C_{84} fullerenes. Different colors correspond to various values of atomic dipole moment.

cones are analyzed which reveals two physical origins: flexoelectricity and edge contribution. The influence of the edge of carbon cones was excluded by connecting two identical individual cones with each other by their edges.

The density functional theory[4,5] within the local density approximation for the exchange-correlation functional[6] employing norm-conserving Troullier–Martins pseudopotentials[7] in the Kleinman–Bylander factorized form[8] was used for calculation of electronic properties of the studied structures. Finite-range numerical pseudoatomic wave functions were used as an atomic-orbital basis set. The geometrically confined systems were treated in a supercell scheme allowing at least 20 Å of empty space between them to make intermolecular interactions negligible. The geometry of the structures was optimized until residual forces became less than 0.04 eV/Å. The real-space mesh cutoff was set to 200 Ry for the relaxation and calculation of dipole moment of whole system and to 350 Ry for the charge density output. The Monkhorst–Pack[9] special k-point scheme was used. The 0.1 $Å^{-1}$ k-point spacing was used during the relaxation. For the electronic structure calculations the SIESTA package[10,11] was used. At the DFT level of theory, the dipole moment of hydrocarbon molecules can be well predicted: values of dipole moment of azulene and toluene are equaled to 0.796 ± 0.014 D[12] (experiment) and 0.813 D (computation) and to 0.360 D[13] (experiment) and 0.357 D (computation), respectively. Therefore, we can expect the same accuracy of the calculation of dipole moment of considered structures.

To calculate the dipole moment assigned to an individual atom, it is necessary to decompose the total charge distribution of the structure into atomic charge cells. In ref 2, such a decomposition procedure was carried out for the carbon nanotubes by Bader method,[14] which splits the whole charge of the system into nonoverlapped regions based on the methodology of zero-flux surface in the gradient of the charge density. In present work, the method of construction of Wigner–Seitz cell for each atom was used. Such a simple and physically clear procedure allows the dividing of charge density obtained from DFT calculations of any crystal lattice to assign the individual charge cell around each atom in the lattice. The Wigner–Seitz decomposition results in electrically neutral atomic cells (within the accuracy of finite grid cut) in all considered systems which is originated from the pure covalent bonding in carbon structures. It allows one to assume that this approach can be used for the evaluation of atomic dipole moment, which was calculated with respect to the center of individual atom where the integration over the cut cell volume was carried out as $\int \rho(\vec{r})\vec{r}\, d^3\vec{r}$. It should be noted that the results of atomic dipole moment calculations obtained by Wigner–Seitz cell and by Bader methods are same. This result underlines the validity of using either Bader or Wigner–Seitz procedures of charge decomposition which are based on the different physical approaches: dividing of electronic density and lattice structure, respectively.

For the estimation of flexoelectric effect in big carbon cones the atomic structures were optimized by molecular mechanics method with AIREBO Brenner/Stuart potential[15] as implemented into LAMMPS package.[16]

The induction of atomic dipole moment by the curvature of the atomic net relates with a loss of plane mirror symmetry of initial structure and with redistribution of charge density. The initial operating assumption is the possibility to assign the dipole moment values to every equivalent atom of the high-symmetry structures: carbon nanotubes, high-symmetry fullerenes (C_{60}, C_{20}, and C_8), and graphene (in the last case all atoms have zero dipole moment). The electronic density of the whole structure is decomposed into atomic charge density cells and atomic dipole moments are evaluated. As in a previous case,[2] the linear dependence of atomic dipole moment on the curvature of the structures was obtained (see inset in Figure 1a), except highly distorted structures of (2,2), (3,0), (4,0) nanotubes and C_8 fullerene. It should be noted that in the case of fullerenes, the curvature value is doubled due to the spherical shape containing two principle Gaussian curvatures,[3] which is different from the cylinder (nanotube). From the approximately linear dependence, the flexoelectric constant f_R = 0.80 D·Å was obtained. The f_R constant determines the relationship between curvature and dipole moment with a value that is very close to the data from ref 2 (0.82 D·Å) and ref 3 (0.75–0.90 D·Å) calculated for the CNT and bent graphene piece, respectively.

We see that curvature is not the only geometrical measure relating to the local dipole moment, per atom. Another convenient measure is pyramidalization angle $\Theta_{\sigma\pi}$, defined as an angle between σ and π orbitals, equaled to $\pi/2$ for planar systems (further, the value $\theta_p = \Theta_{\sigma\pi} - \pi/2$ will be used). Pyramidalization angle is valuable parameter for describing the

DOI: 10.1021/acs.jpclett.5b01041
J. Phys. Chem. Lett. 2015, 6, 2740–2744

local distortions of carbon networks and related to the local properties (strain, chemical activity, etc.).[17,18] The curvature and pyramidalization angle are the parameters of continuum and discrete models of atomic structure, respectively, and the relation between them can be easily written down as

$$\mu = f_{\theta p} \cdot \theta_p = F \cdot æ \tag{1}$$

where $f_{\theta p}$ is angle-dependent flexoelectric constant, θ_p is pyramidalization angle, æ is curvature, and F is the curvature-dependent flexoelectric constant.

In case of CNT, pyramidalization angle could be derived from curvature as $\sin(\theta_p) \approx (d/(4R))$, whereas in a case of fullerene it is twice a larger, for the same radius: $\sin(\theta_p) = (d/(2R))$,[17] where d is the interatomic distance, and R is the radius of CNT or fullerene.

The benefit of using pyramidalization angle is in the possibility to extend the analysis to any carbon system with highly local deformations, not fully captured by the overall curvature. To show this, two fullerenes C_{80} (I_h symmetry) and C_{84} (C_s symmetry) with nonidentical atoms were studied. Their structures and color-coded dipole moment values are shown in Figure 1b. Fullerene C_{80} has 2 nonidentical atoms due to its symmetry (I_h), whereas C_{84} has lower symmetry (C_s) and possess 42 nonidentical atoms in the structure and the same number of incrementally different dipoles. Figure 1a shows that atomic dipoles for all structures are well consistent with linear dependence, with $f_{\theta p}$ = 2.34 D/rad.

Having verified the relationship between local curvature and the dipole moment it induces, one can proceed to using it for larger nanostructures, where directing first-principles computation becomes unaffordable or at least cumbersome. Here, we consider the nanocones, produced in a number of experiments.[19−21] A nanocone consists of a curved graphene sheet (like CNT) and a cap with pentagonal defects (like fullerene), which induce overall curvature of the structure. Highly curved cap distorts electronic density at the top of the cone and should display high dipole moment; it might be used as a source for electron emitting in external field.[22]

Different carbon cones (depending on the number of pentagons[23] at the apex) with nominal apex angles of α = 112.9°, 83.6°, 60.0°, 38.9°, and 19.2° were observed in experiment.[21] Figure 2 shows the cone caps, studied here, and cone schematics with basic notations.

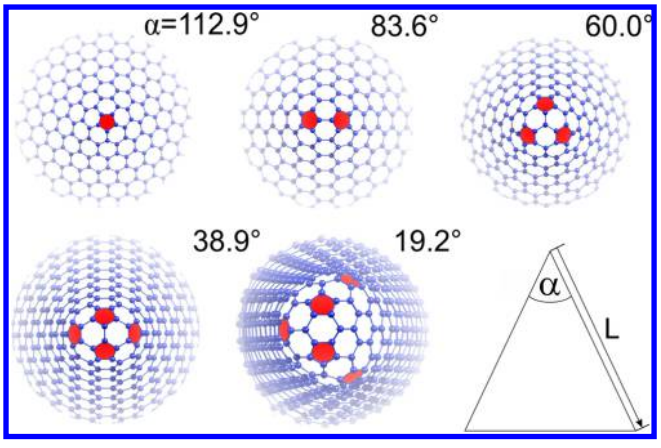

Figure 2. Relaxed structures of the cones with apex angles α = 112.9°, 83.6°, 60.0°, 38.9°, 19.2° and basic schematic showing α and length L.

The total dipole moment of the cone could be divided into three parts. The first one is induced by the curvature of graphene sheet d_{flex} (flexoelectric effect). The second is due to redistribution of charge density near the cone's cap (d_{cap}). Third part is related with the dipole moment of the cone's edge which greatly depends on the passivation type. First, two parts can be computed directly from the pyramidalization angles at each atom, using known $f_{\theta p}$ coefficient. Atoms in the cone's cap will have the greatest individual contribution to the total dipole moment due to the high local curvature. The third edge part is not really intrinsic property of a cone and should be avoided in computations here.

The relation between curvature and dipole moment induced by flexoelectric effect can be established through the integration over the cone surface, that is along its length L

$$d_{\text{flex}} = \frac{1}{S_0}\int_0^{\Delta L} 2\pi R \cdot \frac{f_R}{R} \mathrm{d}z = \frac{\pi}{S_0} f_R \int_0^{\Delta L} \sin(\alpha)\mathrm{d}L \tag{2}$$

Notably, here the mass increment ($\sim R$) and the curvature ($\sim 1/R$) dependencies cancel each other precisely, so that the cumulative dipole moment is simply proportional to linear dimension ($\sim L$) and not to cone area or some complicated function of L

$$d_{\text{flex}}(\Delta L) = \frac{\pi}{S_0} f_R \, \Delta L \sin(\alpha) \tag{3}$$

where S_0 is area per carbon atom (2.62 Å^2) and ΔL is the distance between the apex-cap and the bottom end of the cone. In eq 3, the contribution to the d_{flex} from the cap per se (d_{cap}) is not included but can be added as a constant ($\sim L_0$) obtained from the atomic structure and known $f_{\theta p}$ coefficient.

One can also see from eq 3 how the cone dipole moment depends on the apex angle; the cones with apex angles close to 90° must display the maximum total dipole, among the cones of the same length L. These conclusions are corroborated by atomic-model calculations of the dipole moment depending on the cone's length, shown at Figure 3a. Apex angles equal to 0° and 180° correspond to the limiting cases of the cone with parallel sides which can be represented as (5,5) carbon nanotube (open on one side) or flat graphene, which both do not display any dipole moment, and no dependence on the length. In the former case, only the cap of a tube contributes a constant dipole moment, whereas in the latter case, the dipole moment equals zero. Figure 3b shows the dependence of dipole moment per cone's length on the apex angle depicted by black line. It should be noted that cones with apex angle close to 90° displays the highest value of dipole moment, in accord with analytically derived sine law of eq 3. Further increase of the apex angle leads to the relative reduction of cap's contribution into the total dipole moment.

The derivation of eq 3 is made with the assumption of L = constant, which does not constrain the cone surface (mass), however. Perhaps it is more reasonable to compare the cones of equal mass, which can be done by changing the integration limits in eq 2 from cone length to cone surface ΔS between the end of a cap and end of the cone. Taking $\Delta S = \pi \Delta L^2 \sin(\alpha/2)$ in the above-mentioned integral leads to the equation

$$d_{\text{flex}}(S) = \frac{2\sqrt{\pi}}{S_0} f_R \cos\left(\frac{\alpha}{2}\right)\sqrt{\sin\left(\frac{\alpha}{2}\right)S} \tag{4}$$

One concludes that the maximum dipole moment among the cones of equal surface/mass is shifted to the lower apex angles,

DOI: 10.1021/acs.jpclett.5b01041
J. Phys. Chem. Lett. 2015, 6, 2740−2744

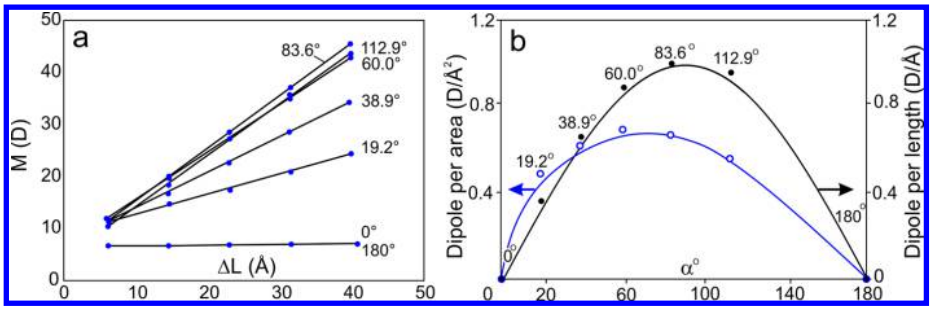

Figure 3. (a) Flexoelectric dipole moments versus the cone length. Dots were obtained by the summation of pyramidalization angles, using $f_{\theta p}$ coefficient. (b) Flexoelectric dipole moment per surface (blue line with empty dots) and per length (black line with filled dots) versus the apex-angle; 0° corresponds to nanotube (5,5) and 180°corresponds to graphene sheet, whose zero values are not shown in (a). Solid black and blue lines represent predicted trends from analytical eqs 3 and 4, respectively.

in comparison with the previous case. Cones with $\alpha \approx 70.5°$ display the largest dipole which leads to the superior dipole moment of "magic" cones with $\alpha = 60.0°$ and 83.6°. The predicted trend is supported by atomistic computations (blue line in Figure 3b) whose values also follow the $\sim \cos(\alpha/2)(\sin(\alpha/2))^{1/2}$ law.

To further validate the results obtained by either continuum level model eq 3 or by the summation $\sum f_{\theta p} \cdot \theta_p$ of pyramidalization contributions over the atomistic structure, we also perform direct DFT computations of the total dipoles. However, to avoid the contribution from the atoms at the cone edge, the symmetrical structure made by joining two identical cones at their edges can be designed (Figure 4a). The dipole moment of individual cone was calculated using the charge density obtained by bisecting the total charge density through symmetry plane (mirror plane or boundary between red and blue regions at Figure 4a). Obtained values of dipole moments for the cones of different apex angles and lengths are shown in Figure 4b, red lines with dots-circles represent results directly from the DFT calculations of charge distribution. Dipole moments obtained from the linear eq 1 between dipole moment and pyramidalization angle are shown by black lines with open squares. The dipole moments calculated by analytical eq 3 are shown by blue lines in Figure 4b and display smaller values of dipole moment compared to other sets, apparently due to omission of the cone's cap contribution. Small difference in the slope can be due to the difference in apex angles of the double symmetrical structure and the nominal angle of a free-individual cone.

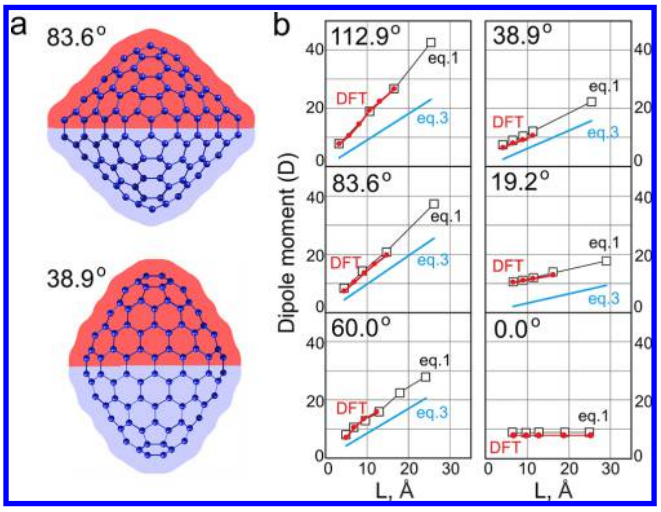

Figure 4. (a) Atomic structures and schematic charge distributions of symmetrical structures corresponding to cones with apex angles of 83.6° and 38.9°. Regions of charge density used for the estimation of dipole moments of each part of double cone in DFT calculations are highlighted by red and blue colors. (b) Flexoelectric dipole moments of the cones depending on their length calculated by different methods. Red lines with circles represent data obtained directly from the calculations of charge distribution; black lines with open squares display data from the linear relation between dipole moment and pyramidalization angle; blue lines show data obtained by using analytical eq 3.

Remarkable agreement between the three sets of data suggests the pure flexoelectric nature of dipole moments in the graphitic cones and demonstrates the power of presented method to predict the flexoelectric dipole moments of arbitrary graphene-based nanostructures directly from their geometry, circumventing the burden of full scale charge density computations, which is often unaffordable. The exclusion of cones edge contribution allows us to obtain the dipole moment originating only from the flexoelectric nature of sp^2 carbon network. Such property of the graphene based nanostructure should reveal itself in every case of bent graphene sheet like in cones or corrugated free-standing graphene even if it is not directly observed in experiment when concealed by other electrostatics (e.g., polar edges).

Presented comprehensive study of flexoelectric effect in carbon nanostructures is based on the ansatz that charge in the covalently bonded structure can be decomposed to be assigned to each individual node-atom (which is rigorous in cases with the atoms identical by symmetry). Extending this from highly symmetrical structures to low-symmetry structures containing nonequivalent atoms allows one to study flexoelectric effect of various carbon nanostructures, for example, carbon cones. It is shown that proposed model describes nanocones with different apex angles and lengths very well, in good agreement with direct full-scale electronic structure computations. The dependence of dipole moment of carbon nanocones on their apex angles and lengths was calculated using empirical relation between dipole moment and pyramidalization angle, and shows perfect agreement between three sets of obtained data: density functional theory approach, empirical linear relation between dipole moment, and local curvature and analytical eq 3. We show a correlation between atomic scale characteristic (pyramidalization angle) and macroscopic characteristic (curvature) of material and substantiate that slight variations in atomic structure will lead to significant changes of

DOI: 10.1021/acs.jpclett.5b01041
J. Phys. Chem. Lett. 2015, 6, 2740−2744

macroscopic characteristics of material by the example of dipole moment.

AUTHOR INFORMATION

Corresponding Authors

*E-mail: pbsorokin@tisnum.ru.
*E-mail: biy@rice.edu.

Notes

The authors declare no competing financial interest.

ACKNOWLEDGMENTS

P.B.S. acknowledges the financial support of the Ministry of Education and Science of the Russian Federation in the framework of Increase Competitiveness Program of NUST ≪MISiS≫ (No K2-2015-033) and Grant of President of Russian Federation for government support of young Ph.D. scientists (MK-6218.2015.2). Authors are grateful to the Moscow State University for access to "Chebyshev" and "Lomonosov" supercomputers; part of the calculations was performed on the Joint Supercomputer Center of the Russian Academy of Sciences. Work at Rice was supported by the US AFOSR MURI Program and in part by the National Science Foundation CMMI (EAGER Grant 0951145).

REFERENCES

(1) Novoselov, K. S.; Jiang, D.; Schedin, F.; Booth, T. J.; Khotkevich, V. V.; Morozov, S. V.; Geim, A. K. *Proc. Natl. Acad. Sci. U.S.A.* **2005**, *102* (30), 10451−10453.
(2) Dumitrica, T.; Landis, C.; Yakobson, B. *Chem. Phys. Lett.* **2002**, *360* (1−2), 182−188.
(3) Kalinin, S. V.; Meunier, V. *Phys. Rev. B* **2008**, *77*, 033403.
(4) Hohenberg, P.; Kohn, W. *Phys. Rev.* **1964**, *136* (3B), B864−B871.
(5) Kohn, W.; Sham, L. J. *Phys. Rev.* **1965**, *140* (4), A1133−A1138.
(6) Perdew, J. P.; Zunger, A. *Phys. Rev. B* **1981**, *23* (10), 5048−5079.
(7) Troullier, N.; Martins, J. L. *Phys. Rev. B* **1991**, *43* (3), 1993−2006.
(8) Kleinman, L.; Bylander, D. *Phys. Rev. Lett.* **1982**, *48* (20), 1425−1428.
(9) Monkhorst, H. J.; Pack, J. D. *Phys. Rev. B* **1976**, *13* (12), 5188−5192.
(10) Ordejón, P.; Artacho, E.; Soler, J. M. *Phys. Rev. B* **1996**, *53* (16), 10441−10444.
(11) Soler, J.; Artacho, E.; Gale, J.; Garcia, A.; Junquera, J.; Ordejon, P.; Sánchez-Portal, D. *J. Phys.: Cond. Mater.* **2002**, *14* (11), 2745−2780.
(12) Tobler, H. J.; Bauder, A.; Günthard, H. H. *J. Mol. Spectrosc.* **1965**, *18* (3), 239−246.
(13) Yaws, C. L. *Thermophysical properties of chemicals and hydrocarbons*; William Andrew: Norwich, NY, 2008. 809 p.
(14) Bader, R F W. *Atoms in Molecules—A Quantum Theory*; Oxford University Press: New York; 1990; p 438.
(15) Stuart, S. J.; Tutein, A. B.; Harrison, J. A. *J. Chem. Phys.* **2000**, *112*, 6472−6486.
(16) Plimpton, S. *J. Comput. Phys.* **1995**, *117* (1), 1−19.
(17) Haddon, R. C. *J. Am. Chem. Soc.* **1997**, *119* (7), 1797−1798.
(18) Hawkins, J. M.; Meyer, A.; Solow, M. A. *J. Am. Chem. Soc.* **1993**, *115* (16), 7499−7500.
(19) Ge, M.; Sattler, K. *Chem. Phys. Lett.* **1994**, *220*, 192−196.
(20) Krishnan, A.; Dujardin, E.; Treacy, M. M. J.; Hugdahl, J.; Lynum, S.; Ebbesen, T. W. *Nature* **1997**, *388* (6641), 451−454.
(21) Naess, S. N.; Elgsaeter, A.; Helgesen, G.; Knudsen, K. D. *Sci. Technol. Adv. Mater.* **2009**, *10* (6), 065002.
(22) Shenderova, O. A.; Lawson, B. L.; Areshkin, D.; Brenner, D. W. *Nanotechnology* **2001**, *12* (3), 191−197.
(23) Smalley, R. E.; Yakobson, B. I. *Solid State Commun.* **1998**, *107*, 597−606.

DOI: 10.1021/acs.jpclett.5b01041
J. Phys. Chem. Lett. 2015, 6, 2740−2744